IEEE Access
Multidisciplinary ⋮ Rapid Review ⋮ Open Access Journal

Received 16 June 2023, accepted 2 July 2023, date of publication 5 July 2023, date of current version 12 July 2023.

*Digital Object Identifier 10.1109/ACCESS.2023.3292542*

RESEARCH ARTICLE

# Detection of Irregular Sheath Current Distribution for Diagnosis of Faults in Grounding Systems of Cross-Bonded Cables

**GEN LI[1], JIE CHEN[2], HONGZE LI[3], LIBIN HU[2], WENJUN ZHOU[1], (Senior Member, IEEE), AND CHENGKE ZHOU[1]**

[1]School of Electrical Engineering and Automation, Wuhan University, Wuhan 430072, China
[2]State Grid Jiangsu Electric Power Company Electric Power Research Institute, Nanjing 211103, China
[3]State Grid Jiangsu Electric Power Company, Nanjing 211103, China

Corresponding author: Chengke Zhou (zhouchengke63@gmail.com)

This work was supported in part by the State Grid under Project 5700-202118195A-0-0-00.

**ABSTRACT** Sheath currents in high voltage cable circuits have proven to be one of the most convenient indicators for assessing cable health. The sheath currents are regularly distributed with fluctuation in a certain range under normal conditions, while the principle of distribution characteristics is still unclear when the cross-bonded grounding system of the cable circuit is abnormal. This paper classifies the common defects of grounding system into three types of circuit topologies and analyzes the correspondence between grounding system conditions and sheath currents. A fault diagnosis method is proposed to detect irregular distribution of sheath currents by quantifying the difference of sheath currents in each of the minor sections and the average currents of each sheath loop. Sensitive analyses are provided to evaluate the criteria, clarifying the influence of fault resistance in each defect. The results show that the method can be very effective when the ratio of the fault resistance to the earth resistance is less than 7.6 for a short-circuit defect in metallic sheath, or less than 1.2 for a short-circuit defect between metallic sheath and ground. The performance of the method is also shown to be very efficient by evaluation with the data collected on site.

**INDEX TERMS** Cable shielding, condition monitoring, current measurement, power cables, fault diagnosis.

## NOMENCLATURE

| | |
|---|---|
| DifCs | The difference sheath currents of a minor section. |
| MS | Minor section. |
| HV | High voltage. |
| Loop 1 | The minor sheath connection A1-B2-C3. |
| Loop 2 | The minor sheath connection B1-C2-A3. |
| Loop 3 | The minor sheath connection C1-A2-B3. |
| MPs | Measuring positions. |
| XLPE | Cross-linked Polyethylene. |

## I. INTRODUCTION

Power cables, which have almost replaced all the traditional overhead transmission lines in urban areas, are the main channel for the transmission and distribution of electricity in cities due to reduced use of land space and high reliability [1], [2], [3]. Urban power grids have the potential to further expand with the increasing penetration of photovoltaic power generation and electric vehicles, which rely on extensive and expensive cable networks for power delivery [4], [5], [6].

Cross bonding is defined in IEEE Standard 575 [7] as a special bonding in which the metallic shields/sheaths of different phase cables in successive minor sections are cross connected in such a way to achieve partial or full cancellation of the induced sheath voltage. Some researchers have investigated numerical models to calculate the sheath currents in normal conditions [8], [9]. Sheath currents depend on the load currents, the installation or laying methods, the length of the cable minor sections, and the external electromagnetic field under normal conditions [10]. Some cable defects cause excessive sheath currents. Researchers attempt to locate the cable insulation faults by sheath currents, while

The associate editor coordinating the review of this manuscript and approving it for publication was Yiqi Liu.

the prerequisite is that the grounding system is in normal condition [11], [12], [13], [14]. The feasibility of detecting a fault in the cable grounding system by monitoring the sheath currents to ground at the end of the cross-bonded sections was presented in [15]. Various criteria were proposed in [12] to detect defects related to open-circuit in metallic sheath loop, breakdown between sheaths, and flooding in link boxes by measuring sheath currents. The defect diagnosis criteria were improved by subtracting the capacitive component of the sheath currents at low load currents with the encoding of the rules [16]. Comparison of the measured and calculated values with historical data was used to assess the condition of the cable grounding system [17]. All the above researches collected currents in the coaxial cable connecting the joints to the cross-link boxes, which are the sum of two sheath loops that have a low correspondence to the defects under abnormal conditions, but diagnostic criteria based on single-loop sheath currents were rarely reported. Previously published methods also required the calculated sheath currents or the data measured under normal conditions as a reference. Significant errors may occur due to difficulties in obtaining accurate parameters for buried or trenched cables. Several researches also attempted to connect the resistors or reactors in the cross-bonding joints to reduce the sheath currents [18], [19]. The aging or deteriorating parts have the potential to expand further and cause serious faults if the defects are no appropriately addressed.

Cable maintenance engineers usually use a clamp meter to measure the amplitude of sheath currents to assess the condition of the grounding system. State Grid Corporation of China standards Q/GDW 456 and Q/GDW 11316 indicates that normal cable circuits should meet the following requirements: a) The absolute value of any sheath current is less than 100A; b) The ratio of any sheath current to load current is less than 20% and has no significant change compared with historical data; c) The ratio of the maximum to minimum sheath current in a cable circuit is less than 3, [10], [20]. A power supply company in southern China classifies a sheath current to load current ratio of greater than 10% but less than 20% as a general defect, and a ratio greater than 20% as a major defect. The sheath currents at each detection point fluctuate within a certain range under normal conditions, while outliers may occur at some detection points under fault conditions. Although the heuristic code of practice is capable of identifying some cable sheath defects, it fails to make full use of the information contained in the sheath currents at all measurement positions. In addition, the standard is unable to provide any preliminary suggestions of the type of a defect from the abnormal sheath currents, it is often difficult for the maintenance engineers to locate and repair the initial defects [21], [22].

This paper analyzes various grounding system conditions and circuit topologies, clarifying the influencing factors of sheath currents which can be measured at each joint under normal conditions and under fault conditions. A fault diagnosis method for grounding systems of cross-bonded cables, quantified by the difference of sheath currents in each of the minor sections and the average currents of the sheath loop, is proposed to detect irregular distribution of the sheath current under different fault topologies. Finally, the performance of the method is evaluated using on site collected data.

## II. THE COMPONENT OF SHEATH CURRENTS

A typical cross-bonded major cable section is shown in Fig. 1. In a major section, there are nine minor metallic sheath sections (A1, A2 …C3), twelve joints (JA0, JB0 …JC3), two cross-bonded link boxes (CB1, CB2), and two grounding boxes (GB1, GB2). At both ends of the major section, the joints are connected, via terminals at the end of the cable circuits, to overhead lines or other plant items, or other cable major sections in the middle of a cable circuit. The metallic sheaths of a major section at both ends are grounded directly through the grounding boxes. The coaxial cables connect the metallic sheaths to the link boxes (CB1, CB2) for the cross-bonded connections. There are three sheath loops in a major section. For brevity, the minor sheath connection A1-B2-C3 is denoted as Loop 1 (red color); the minor sheath connection B1-C2-A3 is denoted as Loop 2 (yellow color); the minor sheath connection C1-A2-B3 (blue color) is denoted as Loop 3. Sheath currents in each sheath loop are composed of leakage currents through the insulation, and induced currents due to the unbalance among the induced voltages in a metallic sheath loop formed by three minor sections

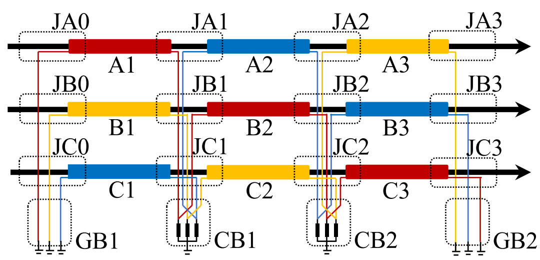


**FIGURE 1. Schematic diagram of a cross-bonded cable major section.**

Maintenance management of HV (high voltage) cables is currently carried out at predetermined intervals, which is known as time-based maintenance. The present schedule of maintenance performs an average inspection of the cable conduit once every 2 weeks (14 days), and an average inspection and test of the remaining cable components every 4 months (120 days) [23]. Cable maintenance engineers usually collect the current of a single sheath loop at a time by opening the link boxes. There are four measuring positions (MPs) in a single sheath loop, resulting in a total of twelve values for three sheath loops in each major section. Taking Loop 1 as an example, the four values are: the $I_{1A}$ for the sheath current of phase A at measuring position 1, $I_{2A}$ for the sheath current of phase A at measuring position 2, $I_{3B}$ for the sheath current of phase B at measuring position 3, and $I_{4C}$ for the sheath current of phase C at measuring position 4, as shown in Figure 2. $l_1$, $l_2$, $l_3$ are the length of each minor section.

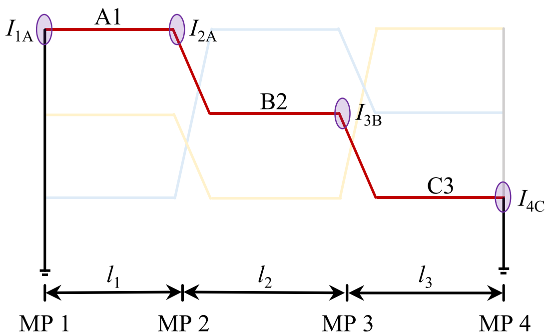


**FIGURE 2. Measurement positions (MPs) of sheath currents in a cross-bonded cable system.**

### A. INDUCED CURRENT

An alternating voltage is induced in the metallic sheath by the alternating load currents during cable operation. As a cable system is always grounded at both ends of each major section for safety, there exist three sheath loops for induced currents as shown in Figure 1. The induced voltages in the metallic sheath are shown in equations (1)-(4) [24].

$$\boldsymbol{U}_i^T = -j\omega \boldsymbol{M}\boldsymbol{I}^T \tag{1}$$

$$\boldsymbol{U}_i = \begin{bmatrix} U_{iA} & U_{iB} & U_{iC} \end{bmatrix} \tag{2}$$

$$\boldsymbol{M} = \begin{bmatrix} L & M_{AB} & M_{AC} \\ M_{AB} & L & M_{BC} \\ M_{AC} & M_{BC} & L \end{bmatrix} \tag{3}$$

$$\boldsymbol{I} = \begin{bmatrix} I_A & I_B & I_C \end{bmatrix} \tag{4}$$

where $\boldsymbol{U}_i$ is the sheath induction voltage matrix, $U_{iA}$, $U_{iB}$, $U_{iC}$ are the induced three phase sheath voltages respectively; $\boldsymbol{M}$ is the mutual inductance matrix, $M_{AB,}$ $M_{AC}$, $M_{BC}$ are the mutual inductance of phase A to phase B, phase A to phase C, and phase B to phase C respectively, $L$ is the inductance of the conductor-to-metal sheath of each phase; $\boldsymbol{I}$ is the load current matrix, $I_A$, $I_B$, $I_C$ are the load currents of three phases; $\omega$ is the angular velocity of the power system.

The induced sheath currents are shown in equations (5)-(7).

$$\boldsymbol{I}_i^T = \frac{1}{Z_s}\boldsymbol{l}\boldsymbol{U}_i^T = -\frac{j\omega}{Z_s}\boldsymbol{l}\boldsymbol{M}\boldsymbol{I}^T \tag{5}$$

$$\boldsymbol{I}_i = \begin{bmatrix} I_{i1} & I_{i2} & I_{i3} \end{bmatrix} \tag{6}$$

$$\boldsymbol{l} = \begin{bmatrix} l_1 & l_2 & l_3 \\ l_3 & l_1 & l_2 \\ l_2 & l_3 & l_1 \end{bmatrix} \tag{7}$$

where $\boldsymbol{I}_{\mathrm{i}}$ is the induced sheath current matrix, $I_{i1}$, $I_{i2}$, $I_{i3}$ are the induced currents on sheath Loop 1, Loop 2, Loop 3, respectively. $\boldsymbol{l}$ is the minor section length matrix, $l_1$, $l_2$, $l_3$ are the lengths of each minor section; $Z_s$ is the sheath circuit impedance.

### B. CAPACITIVE CURRENT

Currents generated by the voltage potential difference between the core conductor and the ground contain capacitive and resistive components. As the insulation resistance of XLPE (Cross-linked Polyethylene) in HV cables can reach hundreds of Giga-Ohms per kilometer, the resistive component would be less than 1 mA/km, while the capacitive component could be several amperes per kilometer. Capacitive currents can be calculated by (8)-(11), [25].

$$\boldsymbol{I}_{\mathrm{c}}^T = -j\omega C \boldsymbol{U}^T \tag{8}$$

$$\boldsymbol{I}_c = \begin{bmatrix} I_{cA} & I_{cB} & I_{cC} \end{bmatrix} \tag{9}$$

$$C = \frac{2\pi\varepsilon_{\mathrm{i}}}{\ln\left(r_{\mathrm{i}}/r_{\mathrm{c}}\right)} \tag{10}$$

$$\boldsymbol{U} = \begin{bmatrix} U_A & U_B & U_C \end{bmatrix} \tag{11}$$

where, $\boldsymbol{I}_c$ is the capacitive current matrix, $I_{cA}$, $I_{cB}$, $I_{cC}$ are capacitive currents in a unit length for each phase respectively; $\boldsymbol{U}$ is the operating voltage matrix, $U_A$, $U_B$, $U_C$ are operating voltages for each phase respectively; $C$ is the capacitance of the main insulation in a unit length, $\varepsilon_i$ is the permittivity of insulation, $r_i$ is the outer diameter of the main insulation; $r_c$ is the outer diameter of the wire core.

### C. INFLUENCING FACTORS OF SHEATH CURRENTS

The factors influencing the sheath current are divided into three main categories, depending on changes in material properties, geometric structure of the cables, and the laying configuration of the cable circuits. The thickness of the insulation and the geometric structure of the metal sheath have an impact on the capacitance parameters and inductance parameters of the conductor-to-metal sheath, which determine the nominal voltage level and the load capacity. The influence of the laying method includes the circuit length, and the phase spacing. The phase spacing directly affects the mutual inductance parameters of the cable circuit. The length of minor sections will directly affect the line capacitance, self-inductance, and mutual inductance parameters. A major impact is the unequal length of minor sections, which result in that the induced voltages in the sheath loop cannot cancel each other out, thus causing a flow of the sheath induction current. After a cable circuit is installed, the change in cable structure and laying configuration can be ignored. The impact of operating environment mainly lies in the applied voltage and load current. The operating voltage is assumed to be a constant vector under normal conditions. The fluctuation of the voltage vector may be negligible in such a scenario. The sheath current fluctuations mainly come from the change in load current.

## III. CHARACTERISTICS AND TOPOLOGIES OF GROUNDING SYSTEMS UNDER NORMAL AND FAULT CONDITIONS

Under normal conditions, the induced voltage in a metal sheath loop is effectively suppressed because their three constituent components are out of phase by 120 degrees.

The sheath current distribution is relatively low at each measurement position. According to the actual circuit parameters in Table 1, distribution characteristics of the sheath currents under normal condition can be calculated using (1)-(11). The results are shown in Figure 3.

**TABLE 1. Main parameters of a cable.**

| Parameter | Value |
|---|---|
| Length of the first minor section $l_1$ /m | 400 |
| Length of the second minor section $l_2$ /m | 450 |
| Length of the third minor section $l_3$ /m | 500 |
| Distance between phase A and B /m | 0.3 |
| Distance between phase B and C /m | 0.3 |
| Distance between phase A and C /m | 0.6 |
| External diameter of the conductor /m | $63.6\times10^{-3}$ |
| External diameter of the insulation /m | $117.8\times10^{-3}$ |
| Voltage rating /kV | 220 |
| Load current /A | 500 |

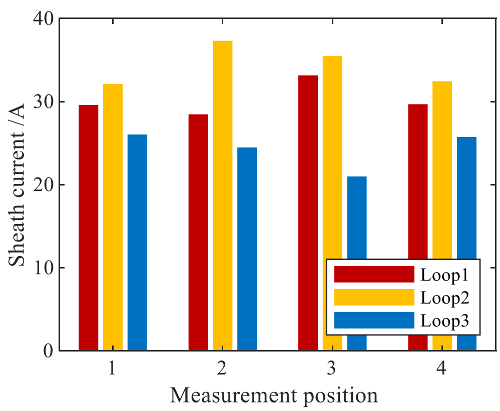


**FIGURE 3. Sheath currents under the normal condition.**

The detected currents are composed of inductive currents and capacitive currents. The inductive currents are the same in one single sheath loop among four measurement positions. The distribution of the capacitive currents determines the differences of the detected currents in the loop under healthy circuit conditions. The inductive currents may be different in circumstances of parallel laying method because the mutual inductances differ among the three phases.

Common faults of cross-connected high-voltage cable sheath and grounding system include open sheath loop, water inlet of cross-connected box, breakdown of epoxy prefabricated connector, damage of outer sheath, and breakdown of sheath overvoltage limiter. Based on the circuit topology, it can be divided into three categories, which are open-circuit in one sheath loop, short-circuit between two sheath loops, short-circuit between a sheath loop and ground. Due to the change of the original circuit topology, the effect of cross-link of metallic sheath, under fault conditions, on balancing out the induced total voltage will be weakened, resulting in unbalanced distribution of sheath currents at some of the measurement points.

### A. OPEN-CIRCUIT IN ONE SHEATH LOOP

The open circuit of high voltage cable sheath is a common grounding system defect. The experience of cable maintenance shows that the open-circuit defects in a sheath loop often appear in the welding of aluminum sheath of high-voltage cable joints and the grounding wire outlet. When the sheath loop open, the cable circuit will lose effective grounding, leading to local temperature rise, suspension potential and other problems, and even insulation failure. Therefore, it is of great significance to identify the open circuit defects in a timely manner.

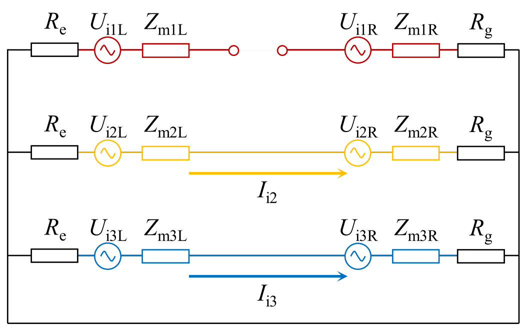


**FIGURE 4. The equivalent circuit of an open-circuit defect in the metallic sheath of Loop 1.**

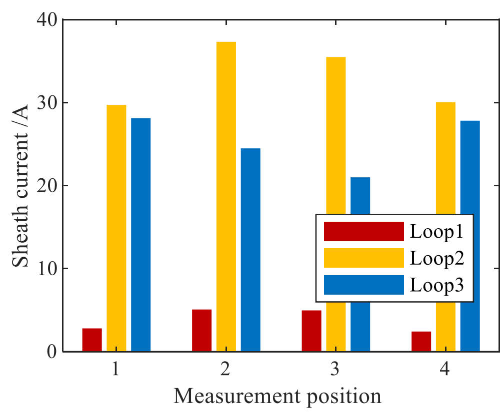


**FIGURE 5. Sheath currents of an open-circuit defect in the metallic sheath of Loop 1.**

There is no induced current in the loop where the open-circuit of the sheath is located. Depending on which of the three sheath loops where the defects occur, it can be divided into three types: open-circuit of the sheath Loop 1, open-circuit of the sheath Loop 2 and open-circuit of the sheath Loop 3. Taking the open-circuit of sheath Loop 1 as an example, the equivalent induction circuit diagram is shown in Figure 4. In the figure, $U_{ixL}$ and $U_{ixR}$ are the total induced voltage of sheath loop $x$ at the left and right sides of the defect point respectively, while $Z_{ixL}$ and $Z_{ixR}$ are the equivalent total impedance of sheath loop $x$ at the left and right sides of the defect point respectively. When an open-circuit defect of the sheath occurs, there is only leakage current in the sheath loop where there is the defect, and the sheath current of the other two circuits is basically unaffected, as shown in Figure 5.

### B. SHORT-CIRCUIT BETWEEN TWO SHEATH LOOPS

Defects corresponding to short circuits between the sheathing circuits often occur inside cable joints. Insulation breakdown can occur at the insulating flange between the metallic sheaths for various reasons, as in Fig. 6. In addition, for the reasons such as the manufacturing process and the installation environment, if there are burrs or impurities between the insulation of the joint sheaths, it may also lead to insulation breakdown between the joint sheaths, and in the worst cases, even to cable joint explosions.

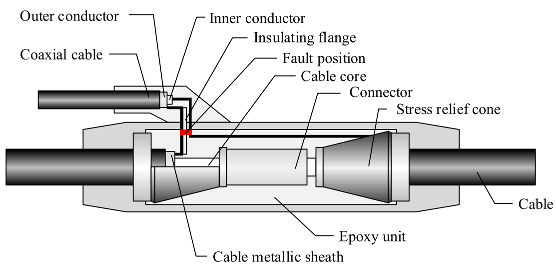


**FIGURE 6. Short-circuit fault in insulating flange.**

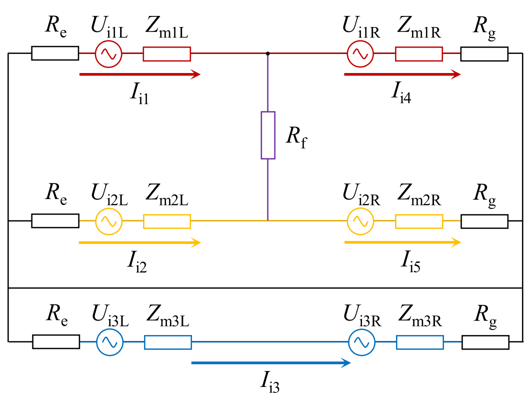


**FIGURE 7. The equivalent circuit of a short-circuit defect in the metallic sheath between Loop 1 and Loop 2.**

Taking a short circuit between sheath Loop 1 and sheath Loop 2 as an example, the equivalent induction circuit is shown in Figure 7. In the figure $R_f$ is the fault resistance, $I_{i1}$ and $I_{i4}$ are the induced currents on both sides of the defective point of sheath circuit 1, and $I_{i2}$ and $I_{i5}$ are the induced currents on both sides of the defective point of sheath circuit 2. After the occurrence of the short circuit defect between two sheath loops, the induced voltage in the two circuits where the defect is located cannot be effectively neutralized, so $I_{i1}$, $I_{i2}$, $I_{i4}$ and $I_{i5}$ have increased compared to those under normal conditions, while the healthy sheath loop current is basically unaffected, as shown in Figure 8.

### C. SHORT-CIRCUIT BETWEEN A SHEATH LOOP AND GROUND

The defects corresponding to the short circuit of the sheath circuit to ground are complex and can be divided into defects

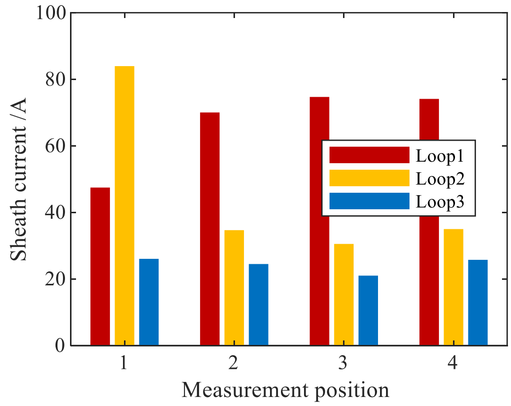


**FIGURE 8. Sheath currents of a short-circuit defect in the metallic sheath between Loop 1 and Loop 2.**

in the metal sheath of the cable body and defects in the cross-interconnection box depending on the location of the defect. The main reason for the defects in the metal sheath of the cable body is that some of the cables are laid in very harsh environment, where moisture, acid and alkaline soil as well as termites or rats may cause the outer sheath of the cable to break down and develop into a multi-point earthing defect. The sheath overvoltage limiter in the cross-connection box can protect the outer sheath insulation from overvoltage damage while the grounding system is operating safely, but after the cable is actually put into operation, it is easy for the isolation switch to be incompletely closed causing overvoltage and other reasons leading to the sheath protector breakdown. The carbonization channel formed by the sheath overvoltage limiter breakdown can be equated to a small resistance earth in the sheath circuit. In addition, during the annual rainy season, high voltage cables installed in cable tunnels can be flooded for months. In the case of poorly sealed cross-connector boxes, the metal parts of the box may be shorted by water, resulting in a short to earth defect in the three metal sheath loops.

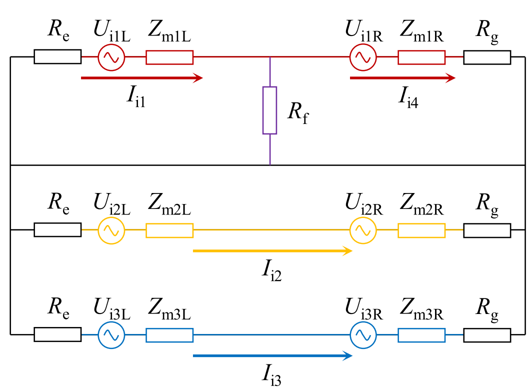


**FIGURE 9. The equivalent circuit of a short-circuit defect between metallic sheath and ground.**

The equivalent circuit of a short-circuit defect between the sheath Loop 1 and ground is shown in Figure 9.

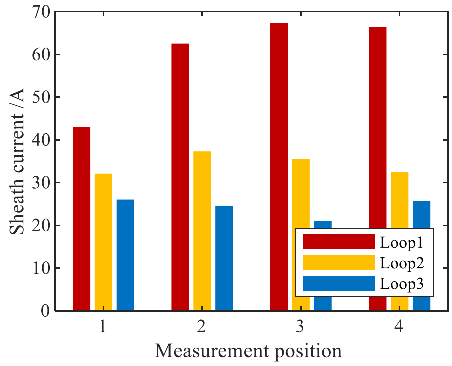


**FIGURE 10. Sheath currents of a short-circuit defect between metallic sheath and ground.**

The neutralization of the induced voltage in the defective sheath loop has been disrupted by the appearance of the new branch. The sheath current in the defective loop becomes excessive, while the currents in the other two loops are basically unaffected, as in Figure 10.

## IV. DIAGNOSTIC CRITERIA AND CASE STUDY

The preceding section examined three categories of defect topologies and their respective sheath current distribution characteristics. This section contrasts the differences among the individual sheath currents and their mean values. The irregular distribution of the sheath current under various defects are then used to propose an effective method for diagnosing of aforementioned cable sheath faults.

### A. UNBALANCED CHARACTERISTICS OF SHEATH CURRENTS

The sheath loops are isolated from each other between grounding boxes at either end of a major section. The mean value of sheath currents in a loop are excessive due to the unbalance among the induced voltages from three minor sections when a new branch appears due to a fault in the loop. There is also an obvious difference between the two sheath currents on either side of the new branch resulting from the different component of the induced voltages on each side. Taking sheath Loop 1 as an example, the difference currents are shown in (12)-(14). Where, $I_{\mathrm{A1}}$, $I_{\mathrm{B2}}$, $I_{\mathrm{C3}}$ are difference currents of each minor sections in Loop 1. $I_{\mathrm{AVE1}}$ is the average current in Loop 1 as in (15). There are nine difference currents and three mean currents in each major section of the cable circuit.

$$I_{\mathrm{A1}} = I_{1\mathrm{A}} - I_{2\mathrm{A}} \tag{12}$$

$$I_{\mathrm{B2}} = I_{2\mathrm{A}} - I_{3\mathrm{B}} \tag{13}$$

$$I_{\mathrm{C3}} = I_{3\mathrm{B}} - I_{4\mathrm{C}} \tag{14}$$

$$I_{\mathrm{AVE1}} = \frac{I_{1\mathrm{A}} + I_{2\mathrm{A}} + I_{3\mathrm{B}} + I_{4\mathrm{C}}}{4} \tag{15}$$

### B. CRITERIA

Define $k_1$ as the difference coefficient and $k_2$ as the mean coefficient to evaluate the irregular current distribution of the sheath loops. The distribution characteristics of the sheath currents under normal and fault conditions are summarized in Table 2. According to Kirchhoff's current law, the difference current obtained by subtracting the sheath currents at the two ends of a minor section are less than the leakage current generated in the segment. The difference coefficient $k_1$ is formulated in (16). Where $k_{th}$ is the threshold coefficient for the margin. $I_{lA}$, $I_{lB}$, $I_{lC}$ are leakage currents calculated by (8)-(11). The mean coefficient is formed in (17) with the consideration that the average value of the sheath loops is primarily affected by the lengths of each minor section under normal conditions. The threshold coefficient $k_{th}$ is recommended as 2.

$$k_1 = k_{th} \cdot \max\{I_{lA}, I_{lB}, I_{lC}\} \cdot \max\{l_1, l_2, l_3\} \tag{16}$$

$$k_2 = k_{th} \frac{\max\{l_1, l_2, l_3\} - \min\{l_1, l_2, l_3\}}{\min\{l_1, l_2, l_3\}} \tag{17}$$

**TABLE 2. Irregular sheath currents under fault conditions and diagnostics criteria.**

| Status | Characteristics | Formulas |
|---|---|---|
| Normal condition | Normal difference | $I_{\mathrm{A1}} < k_1$,<br>$I_{\mathrm{B1}} < k_1$,<br>$I_{\mathrm{C1}} < k_1$,<br>… |
| | Normal mean | $(1\text{-}k_2)\times I_{\mathrm{AVE2}} < I_{\mathrm{AVE1}} < (1+k_2)\times I_{\mathrm{AVE2}}$,<br>$(1\text{-}k_2)\times I_{\mathrm{AVE1}} < I_{\mathrm{AVE2}} < (1+k_2)\times I_{\mathrm{AVE1}}$,<br>… |
| Open-circuit in a loop | Normal difference | $I_{\mathrm{A1}} < k_1$,<br>$I_{\mathrm{B1}} < k_1$,<br>$I_{\mathrm{C1}} < k_1$,<br>… |
| | One mean value is small | $I_{\mathrm{AVE1}} < (1\text{-}k_2)\times I_{\mathrm{AVE2}}$,<br>$I_{\mathrm{AVE1}} < (1\text{-}k_2)\times I_{\mathrm{AVE3}}$;<br>$(1\text{-}k_2)\times I_{\mathrm{AVE3}} < I_{\mathrm{AVE2}} < (1+k_2)\times I_{\mathrm{AVE3}}$,<br>$(1\text{-}k_2)\times I_{\mathrm{AVE2}} < I_{\mathrm{AVE3}} < (1+k_2)\times I_{\mathrm{AVE2}}$; |
| Short circuit between two sheath loops | Two difference values are large | $I_{\mathrm{A1}} > k_1$,<br>$I_{\mathrm{C1}} > k_1$;<br>$I_{\mathrm{B1}} < k_1$,<br>$I_{\mathrm{A2}} < k_1$,<br>$I_{\mathrm{B2}} < k_1$,<br>… |
| | One mean value is small | $I_{\mathrm{AVE2}} < (1+k_2)\times I_{\mathrm{AVE1}}$,<br>$I_{\mathrm{AVE2}} < (1+k_2)\times I_{\mathrm{AVE3}}$;<br>$(1\text{-}k_2)\times I_{\mathrm{AVE3}} < I_{\mathrm{AVE1}} < (1+k_2)\times I_{\mathrm{AVE3}}$,<br>$(1\text{-}k_2)\times I_{\mathrm{AVE3}} < I_{\mathrm{AVE3}} < (1+k_2)\times I_{\mathrm{AVE3}}$; |
| Short circuit between a sheath loop and ground | One difference value is large | $I_{\mathrm{A1}} > k_1$;<br>$I_{\mathrm{B1}} < k_1$,<br>$I_{\mathrm{C1}} < k_1$,<br>… |
| | One mean value is large | $(1+k_2)\times I_{\mathrm{AVE2}} < I_{\mathrm{AVE1}}$,<br>$(1+k_2)\times I_{\mathrm{AVE3}} < I_{\mathrm{AVE1}}$;<br>$(1\text{-}k_2)\times I_{\mathrm{AVE3}} < I_{\mathrm{AVE2}} < (1+k_2)\times I_{\mathrm{AVE3}}$,<br>$(1\text{-}k_2)\times I_{\mathrm{AVE2}} < I_{\mathrm{AVE3}} < (1+k_2)\times I_{\mathrm{AVE2}}$; |

### C. SENSITIVITY ANALYSIS

The fault resistance affects the difference of sheath currents in the sheath-to-sheath short-circuit defects and the sheath-to-ground short-circuit defects. Since the resistance of metallic sheath is small compared to the ground resistance, the ratio of the fault resistance to the ground resistance is regarded as an indicator. The sensitivity of the criteria is represented by the relationship between the ratio of the fault resistance to the ground resistance and the difference of the sheath currents. The influence of the fault resistance for short-circuit faults between sheath loops is shown in Figure 11. The difference of the sheath currents can be detected as abnormal when the ratio of the fault resistance to the ground resistance is less than 7.6 with the proposed method. The influence of the fault resistance for the sheath-to-ground short-circuit defects is shown in Figure 12. The difference of the sheath currents can be detected as abnormal when the ratio of the fault resistance to the ground resistance is less than 1.2.

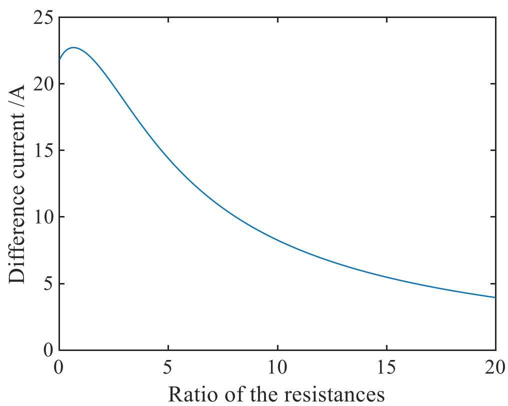


**FIGURE 11.** Short circuit between sheath loops influenced by fault resistance.

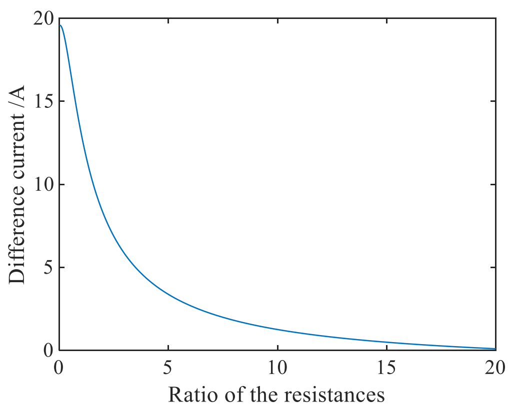


**FIGURE 12.** Short-circuit defect between metallic sheath and ground influenced by fault resistance.

### D. CASE STUDY

In order to verify the validity of the above method, this paper collects the data from several cable circuits in southern China.

These cable circuits are constructed by using XLPE cables with a cross-section of 2500 mm$^2$ and operate at a voltage level of 220 kV. The four measurement positions in the major section are labeled from #9 to #12. The lengths of the minor sections are 477 m, 503 m and 449 m. The phase spacing is unknown because the cable circuit was established decades ago using a mixture of buried and trenched layouts. The field data are presented in Table 3.

**TABLE 3.** Measurement of Sheath Currents in Case 1.

| Date | Position | Sheath current /A | | |
|---|---|---|---|---|
| | | Phase A | Phase B | Phase C |
| 2021.09.24 | #9 | 11.4 | 15.9 | 20.9 |
| | #10 | 13.5 | 30.3 | 30.5 |
| | #11 | 15.4 | 6.4 | 11.4 |
| | #12 | 15.4 | 20.4 | 9.4 |
| 2022.03.21 | #9 | 11.6 | 14.8 | 20.9 |
| | #10 | 12.5 | 28.9 | 30.4 |
| | #11 | 14.5 | 5.6 | 11.3 |
| | #12 | 12.6 | 18.5 | 9.5 |
| 2022.06.29 | #9 | 11.6 | 14.8 | 20.9 |
| | #10 | 16.5 | 25.6 | 28.9 |
| | #11 | 13.6 | 7.8 | 12.5 |
| | #12 | 16.5 | 13.6 | 9.5 |
| 2022.08.19 | #9 | 12.3 | 15.2 | 18.9 |
| | #10 | 15.8 | 21.5 | 28.9 |
| | #11 | 13.5 | 8.3 | 11.5 |
| | #12 | 14.6 | 13.5 | 8.4 |

The difference currents (DifCs) of each minor section (MS) and the mean currents of the three loops are calculated by (12)-(15) with the average sheath currents at each measurement position derived from Table 3, as in Figure 13. The difference coefficient $k_1$ is 12.06 A and the mean coefficient $k_2$ is 0.21, obtained from (16)-(17). The difference currents of A3 and B3 are abnormal with the excessive mean currents of Loop2 and Loop3. It is assumed that there is a short circuit in the #7 joint according to the criteria in Table 2. The insulation resistances of each minor section and joint are measured as in Table 4. It is suspected that there is a breakdown in the insulation at joint #7.

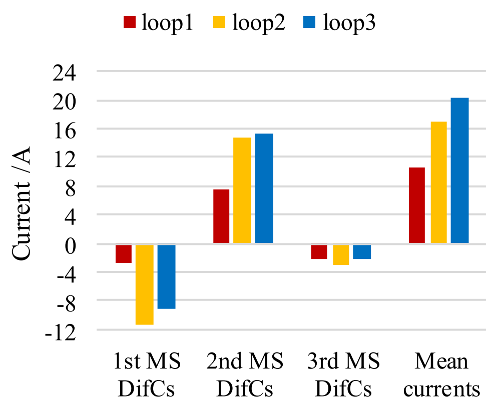


**FIGURE 13.** The difference currents (DifCs) of each minor section (MS) and the mean currents of the three loops measured in Case I.

Sheath currents of another cable circuit in the vicinity with the same configuration are illustrated as in Figure 14. The difference current of the second minor section in Loop3 is abnormal with the excessive mean currents of Loop3. It is

**TABLE 4. Insulation resistance testing.**

| Position | Insulation resistance (applied 500 V) /MΩ | | |
|---|---|---|---|
| | Phase A | Phase B | Phase C |
| #9-#10 Minor section | 31 | 105 | 0.05 |
| #10-#11 Minor section | 35.5 | 30 | 51 |
| #11-#12 Minor section | 32.9 | 200 | 280 |
| #10 Joint | 62.5 | 95 | 44.7 |
| #11 Joint | Less than 0.01 | 63.7 | 95.8 |

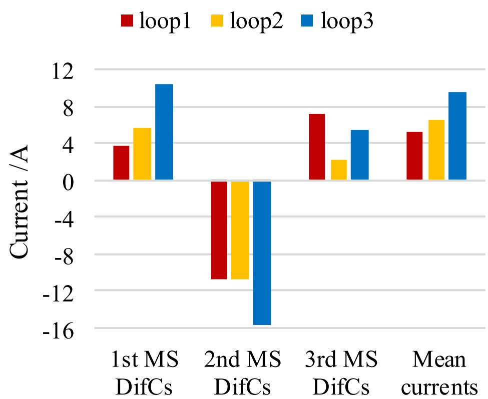


**FIGURE 14. The difference currents (DifCs) of each minor section (MS) and the mean currents of the three loops measured in Case II.**

roughly concluded that there is a multi-point ground fault due to the damaged outer jacket in the A phase at the second minor section. This was confirmed after the cable circuit inspection.

## V. DISCUSSION AND CONCLUSION

This paper proposes a novel sheath fault diagnosis method for cross-bonded HV cable grounding system, which represents an improvement to the existing standards. It is intended to help maintenance engineers make preliminary decisions for locating and repairing the initial defects.

Defects in the earthing system of cross-bonded cables may cause irregular distribution of the sheath currents, which can be used to identify the topologies of the sheath loops. The unbalanced distribution of the sheath currents can be quantified by the difference values and the mean values derived from the data collected at four measurement positions in each major section. The criteria established by the difference coefficient and the mean coefficient are proven to have a good performance for fault diagnosis with field data.

It is to be noted that only limited amount of validation work has been carried out so far. Further research and improvement may be required on further types of faults. More validations will be conducted when more on site data becomes available.

## REFERENCES

[1] C. Zhou, H. Yi, and X. Dong, "Review of recent research towards power cable life cycle management," *High Voltage*, vol. 2, no. 3, pp. 179–187, Sep. 2017.

[2] Z. Tang, C. Zhou, W. Jiang, W. Zhou, X. Jing, J. Yu, B. Alkali, and B. Sheng, "Analysis of significant factors on cable failure using the cox proportional hazard model," *IEEE Trans. Power Del.*, vol. 29, no. 2, pp. 951–957, Apr. 2014.

[3] Z. Tang, W. Zhou, J. Zhao, D. Wang, L. Zhang, H. Liu, Y. Yang, and C. Zhou, "Comparison of the Weibull and the crow-AMSAA model in prediction of early cable joint failures," *IEEE Trans. Power Del.*, vol. 30, no. 6, pp. 2410–2418, Dec. 2015.

[4] M. M. F. Darwish, M. H. A. Hassan, N. M. K. Abdel-Gawad, and D. A. Mansour, "Application of infrared spectroscopy for discrimination between electrical and thermal faults in transformer oil," in *Proc. 9th Int. Conf. Condition Monitor. Diagnosis (CMD)*, Nov. 2022, pp. 255–258.

[5] M. M. F. Darwish, M. H. A. Hassan, N. M. K. Abdel-Gawad, and D. A. Mansour, "A new method for estimating transformer health index based on ultraviolet-visible spectroscopy," in *Proc. 23rd Int. Middle East Power Syst. Conf. (MEPCON)*, Dec. 2022, pp. 1–5.

[6] M. Badawi, S. A. Ibrahim, D. A. Mansour, A. A. El-Faraskoury, S. A. Ward, K. Mahmoud, M. Lehtonen, and M. M. F. Darwish, "Reliable estimation for health index of transformer oil based on novel combined predictive maintenance techniques," *IEEE Access*, vol. 10, pp. 25954–25972, 2022.

[7] *IEEE Guide for Bonding Shields and Sheaths of Single-Conductor Power Cables Rated 5 kV Through 500 kV*, IEEE Standard 575-2014, 2014.

[8] J. S. Barrett and G. J. Anders, "Circulating current and hysteresis losses in screens, sheaths and armour of electric power cables—Mathematical models and comparison with IEC standard 287," *IEE Proc.-Sci., Meas. Technol.*, vol. 144, no. 3, pp. 101–110, May 1997.

[9] A. H. M. Arnold, "The theory of sheath losses in single-conductor lead-covered cables," *J. Inst. Electr. Eng.*, vol. 67, no. 384, pp. 69–89, Dec. 1928.

[10] Y. Lin and Z. Xu, "Cable sheath loss reduction strategy research based on the coupled line model," *IEEE Trans. Power Del.*, vol. 30, no. 5, pp. 2303–2311, Oct. 2015.

[11] T. Lan, S. M. Mazhari, H. Teimourzadeh, and C. Y. Chung, "An online data-efficient HV cable fault localization approach via an AI-enabled recognition of modal wavefront in sheath current," *IEEE Trans. Power Del.*, vol. 38, no. 3, pp. 1977–1989, Jun. 2023.

[12] X. Wang, J. Yong, and L. Li, "Investigation on the implementation of the single-sheath bonding method for power cables," *IEEE Trans. Power Del.*, vol. 37, no. 2, pp. 1171–1179, Apr. 2022.

[13] Z. Tang, P. Zhang, R. Liang, N. Peng, M. Cheng, and Y. Qiao, "Permanent fault location for three-core cable using multiconductor coupling model," *IEEE Trans. Power Del.*, vol. 37, no. 2, pp. 1120–1129, Apr. 2022.

[14] L. Li, J. Yong, and W. Xu, "Single-sheath bonding—A new method to bond/ground cable sheaths," *IEEE Trans. Power Del.*, vol. 35, no. 2, pp. 1065–1068, Apr. 2020.

[15] M. Marzinotto and G. Mazzanti, "The feasibility of cable sheath fault detection by monitoring sheath-to-ground currents at the ends of cross-bonding sections," *IEEE Trans. Ind. Appl.*, vol. 51, no. 6, pp. 5376–5384, Nov./Dec. 2015.

[16] X. Dong, Y. Yang, C. Zhou, and D. M. Hepburn, "Online monitoring and diagnosis of HV cable faults by sheath system currents," *IEEE Trans. Power Del.*, vol. 32, no. 5, pp. 2281–2290, Oct. 2017.

[17] M. A. Shokry, A. Khamlichi, F. Garnacho, J. M. Malo, and F. Álvarez, "Detection and localization of defects in cable sheath of cross-bonding configuration by sheath currents," *IEEE Trans. Power Del.*, vol. 34, no. 4, pp. 1401–1411, Aug. 2019.

[18] Z. Li, B. Du, and W. Li, "Evaluation of high-voltage AC cable grounding systems based on the real-time monitoring and theoretical calculation of grounding currents," *High Voltage*, vol. 3, no. 1, pp. 38–43, Mar. 2018.

[19] S. Huang, X. Liu, W. Su, and S. Yang, "Application of hybrid firefly algorithm for sheath loss reduction of underground transmission systems," *IEEE Trans. Power Del.*, vol. 28, no. 4, pp. 2085–2092, Oct. 2013.

[20] *Guide for Condition Evaluation of Power Cable*, Standard Q/GDW 456, State Grid Corporation of China, 2010.

[21] *Test Code for HV Power Cables*, Standard Q/GDW 11316, State Grid Corporation of China, 2018.

[22] J. Yuan, W. Zhou, X. Xu, Y. Liao, and C. Zhou, "Time-delay concept-based approach to maintenance scheduling of HV cables," *High Voltage*, vol. 5, no. 6, pp. 724–730, Dec. 2020.

[23] Y. Liao, H. Liu, J. Yuan, Y. Xu, W. Zhou, and C. Zhou, "A holistic approach to risk-based maintenance scheduling for HV cables," *IEEE Access*, vol. 7, pp. 118975–118985, 2019.

[24] M. Li, C. Zhou, and W. Zhou, "A revised model for calculating HV cable sheath current under short-circuit fault condition and its application for fault location—Part 1: The revised model," *IEEE Trans. Power Del.*, vol. 34, no. 4, pp. 1674–1683, Aug. 2019.
[25] Y. Yang, D. M. Hepburn, C. Zhou, W. Zhou, and Y. Bao, "On-line monitoring of relative dielectric losses in cross-bonded cables using sheath currents," *IEEE Trans. Dielectr. Electr. Insul.*, vol. 24, no. 5, pp. 2677–2685, Oct. 2017.

**GEN LI** was born in China. He received the B.Sc. degree from the Huazhong University of Science and Technology, Wuhan, China, in 2017, and the master's degree from the Wuhan Research Institute of Post and Telecommunication, Wuhan, in 2021. He is currently pursuing the Ph.D. degree with Wuhan University, Wuhan. His current research interests include fault location and condition monitoring of power cables.

**JIE CHEN**, photograph and biography not available at the time of publication.

**HONGZE LI**, photograph and biography not available at the time of publication.

**LIBIN HU**, photograph and biography not available at the time of publication.

**WENJUN ZHOU** (Senior Member, IEEE) was born in China, in July 1959. He received the Ph.D. degree in hydraulic and electrical engineering from the Wuhan University of Hydraulic and Electrical Engineering, Wuhan, China, in 1990. He is currently a Professor with the School of Electrical Engineering and Automation, Wuhan University. He is also the Vice Director of the Hubei High Voltage Committee. His current research interests include lightning protection and diagnostic techniques for outdoor electrical insulations. He is a member of the High Voltage Committee, Chinese Society of Electrical Engineering (CSEE); the Electrotechnical Test and Measurement Committee, China Electro-Technical Society (CES); and the China Lightning Protection Standard Committee.

**CHENGKE ZHOU** received the B.Sc. and M.Sc. degrees in electrical engineering from the Huazhong University of Science and Technology, China, in 1983 and 1986, respectively, and the Ph.D. degree from the University of Manchester, U.K., in 1994. Since 1994, he has been a Lecturer with Glasgow Caledonian University (GCU). He was a Reader with Heriot-Watt University, in 2006. In 2007, he returned to GCU, as a Professor. He is currently a Visiting Professor with the School of Electrical Engineering, Wuhan University. He has published more than 180 articles in the area of PD-based condition monitoring of MV/HV plants and power system analysis. He is a fellow of the IET.